Journal of Applied Mathematics and Physics, 2022, 10, 1910-1917
https://www.scirp.org/journal/jamp
ISSN Online: 2327-4379
ISSN Print: 2327-4352

Internal Flow Field Measurement of Gas Turbine Based on Optical Flow Method

Chengyang Li

University of Shanghai for Science and Technology, Shanghai, China
Email: 2629393448@qq.com

How to cite this paper: Li, C.Y. (2022) Internal Flow Field Measurement of Gas Turbine Based on Optical Flow Method. *Journal of Applied Mathematics and Physics*, **10**, 1910-1917.
https://doi.org/10.4236/jamp.2022.106131

Received: May 18, 2022
Accepted: June 21, 2022
Published: June 24, 2022

Abstract

The in-cylinder flow field of the internal combustion engine is an important factor affecting the quality and combustion quality of the fuel mixture in the cylinder. In order to calculate the high-precision flow field, the paper presents a flow field calculation method based on the optical flow algorithm. The motion of the point was calculated using the change in pixel intensity within two temporally adjacent frame images. The results show the high accuracy and resolution of the flow field at small displacement conditions.

Keywords

Optical Flow Method, Particle Image Velocity Measurement, Flow Field Calculation

1. Introduction

The internal combustion engine is widely used in various fields of the national economy, which is the key equipment of the energy and power industry, and is also the core component of aviation power engineering. The flow in gas turbines (including air and gas) is extremely complex. The flow in the compressor due to pressurized flow may stall flow and develop into a surge, endangering the safety of the gas turbine. In the turbine flow, the cooling working medium is injected and mixed with the main stream, which may cause the local thermal fatigue fracture of the blade. The high-speed relative motion between the multi-stage compressor and the static and static grille of the turbine may cause airflow-induced blade vibration and endanger the blade's safety. The solution to these problems depends on our understanding of the correlated flow phenomena. For the test of gas turbine flow field, there are many forming algorithms. Liu You from Harbin Engineering University proposed the flow field test technology

based on laser Doppler technology, using the laser Doppler effect for flow velocity measurement [1]. Yang Yanxiang, Wang Tianyu, *et al.* from Tianjin University used the autocorrelation-based particle image velocimetry technology to determine the full-field flow velocity distribution of the flow field in the combustion cylinder of a certain moment [2]. Bruce D. Lucas and Takeo Kanade proposed to treat the tracer particle as a stream of particles, and proposed that the change of the gray value of the two sequences is linear changes to track the particles and get the motion field [3]. Theo Benkovic derived a new particle tracking algorithm based on the merger method with the aim to overcome the current limitations of high particle density flows. The method integrates the matching probability-based relaxation algorithm into the vision-based concept of feature association and achieves good results [4]. The most adopted method is based on the particle image velocimetry of cross-correlation, which determines the position of the matching region through the peak of the cross-correlation function, and then obtains the displacement field [5]. Subsequently, Bao Xiaoli *et al.* from Dalian University of Technology adopted the cross-correlation algorithm based on the fast Fourier transform and improved it [6]. Nie Mingyuan proposed a particle tracking velocimetry based on a mixed ant colony algorithm, using an improved ant colony optimization to find the minimized global solution of the particle matching function to obtain the matching particles [7]. These methods have achieved good results for flow field testing, but when the density of tracer particles inside the internal combustion engine is relatively large, these methods cannot accurately calculate the flow field with high accuracy. In this paper, a method combining a Gaussian pyramid to calculate optical flow is proposed. First, an interpolation method is used to build different resolution images for each frame, with the original image at the bottom and the highest resolution image at the top. Starting from the top layer, the optical flow of each point is calculated as the input of the next layer, and the finally obtained high-resolution optical flow field is used as the displacement field.

2. Optical Flow Method

2.1. Physical Significance of Optical Flow

Optical flow was first proposed by Gibson to describe the speed of image motion [8]. When the human eye looks at a moving object, the scene of the object forms a series of continuous changing images on the retina of the human eye. This series of continuous changing information constantly "flows" through "the retina" (namely the image plane), like a "flow" of light, so it is called light flow. Optical flow expresses the change in the image, and because it contains information about the movement of the target, it can be used by observers to determine the movement of the target [9].

In space, the movement can be described by the motion field, and in an image plane, the movement of the object is often reflected by the different image gray scale distribution in the image sequence, so that the sports field in the space is

transferred to the image is represented as the optical flow field (optical flow field). The optical flow field is a two-dimensional vector field that reflects the changing trend of every point of gray degree on the image. It can be regarded as the instantaneous velocity field generated by the motion of pixels with gray degree in the plane of the image. It contains information that is the instantaneous motion velocity vector information of each image point. The purpose of studying optical flow fields is to approximate the motion fields that cannot be directly obtained from sequence images. Optical flow field in the ideal case, the optical flow field corresponds to the sports field [10].

2.2. Basic Principles of Optical Flow Field Calculation

At time t, the gray value at the pixel (x, y) is $I(x, y, t)$ and at $(t+\Delta t)$, the point moves to a new position, its position on the image is ($x+\Delta x$, $y+\Delta y$), the grayscale value is recorded as $I(x+\Delta x, y+\Delta y)$. According to the image consistency assumption, the brightness of the image remains constant along the motion trajectory [11] [12], it can be obtained that:

$$I(x, y, t) = I(x+\Delta x, y+\Delta ytz+\Delta t) \tag{1}$$

Assume that and are the two components of the optical flow vector at this point along the direction of and respectively. Then, expand the right side of Equation (1) by Taylor formula, and obtain: $\mu = \mathrm{d}x/\mathrm{d}t, \nu = \mathrm{d}y/\mathrm{d}t$

$$I(x+\Delta x, y+\Delta y, t+\Delta t) = I(x, y, t) + \frac{\partial I}{\partial x}\Delta x + \frac{\partial I}{\partial y}\Delta y + \frac{\partial I}{\partial t}\Delta t \tag{2}$$

Ignore higher order terms of more than second order, then:

$$\frac{\partial I}{\partial x}\Delta x + \frac{\partial I}{\partial y}\Delta y + \frac{\partial I}{\partial t}\Delta t = 0 \tag{3}$$

$$\frac{\partial I}{\partial x}\frac{\mathrm{d}x}{\mathrm{d}t} + \frac{\partial I}{\partial y}\frac{\mathrm{d}y}{\mathrm{d}t} + \frac{\partial I}{\partial t}\frac{\mathrm{d}t}{\mathrm{d}t} = 0 \tag{4}$$

That is:

$$I_x\mu + I_y\nu + I_t = 0 \tag{5}$$

Equation (5) is the basic equation of optical flow, where I_x, I_y and I_t are the partial derivatives of the gray value of the reference point pixel along the x, y and t directions. The basic idea of additional constraints cited by Horn-Schunck algorithm is that when solving optical flow, the optical flow itself should be as smooth as possible, that is, the whole smoothness constraint of optical flow is introduced to solve ill-conditioned optical flow equation. The so-called smooth, is in a given neighborhood $\left(\nabla^2\mu + \nabla^2\nu\right)$ should be reduced as much as possible, and this is the constraint condition to find the extreme value of the condition. The conditions attached to μ and ν are as follows:

$$\min\left\{\left(\frac{\partial\mu}{\partial x}\right)^2 + \left(\frac{\partial\mu}{\partial y}\right)^2 + \left(\frac{\partial\nu}{\partial x}\right)^2 + \left(\frac{\partial\nu}{\partial y}\right)^2\right\} \tag{6}$$

In Formulas (5) and (6) H-S optical flow method, the calculation of μ and v is summarized as follows:

$$\min\left\{\iint\left(I_x+I_y+I_t\right)^2+\alpha^2\left[\left(\frac{\partial\mu}{\partial x}\right)^2+\left(\frac{\partial\mu}{\partial y}\right)^2+\left(\frac{\partial v}{\partial x}\right)^2+\left(\frac{\partial v}{\partial y}\right)^2\right]\right\} \tag{7}$$

Therefore, the corresponding Euler-Lagrange equation can be obtained and solved by gauss-Seidel method. The first to $(n+1)$ iterations of each sub-position of the image can be estimated as:

$$\mu^{n+1}=\mu^n-I_x^2\frac{I_x\mu^n+I_yv^n+I_t}{\alpha^2+I_x^2+I_y^2} \tag{8}$$

$$\mu^{n+1}=\mu^n-I_{yx}^2\frac{I_x\mu^n+I_yv^n+I_t}{\alpha^2+I_x^2+I_y^2} \tag{9}$$

The solution process usually requires hundreds of iterations to arrive at a stable solution. The whole iteration process is related to both the image size and the amount of transfer (speed change) each time. According to the iterative formula, it can be found that in some regions lacking features and relatively flat (with a gradient of 0 or smaller), the velocity is determined by the first term of the iterative formula, and the velocity information of this point needs to be transmitted from the region with rich features. In order to accelerate the convergence speed of the algorithm, on the one hand, the pyramid hierarchy can be used to reduce the size diffusion of the image; on the other hand, the method of increasing the diffusion can be used to accelerate the algorithm [13].

3. Implementation Step

1) Image preprocessing, mainly including Gaussian filtering, binarized images, building a hybrid Gaussian model for foreground extraction to reduce environmental changes to the measurement of flow field accuracy.

2) Gradients in the image *x*, *y*, and *t* directions were calculated. Calculation method: Half of the gray scale difference of two adjacent pixels along the direction of *x* and *y*. Calculation method: The pixel gray scale difference between the corresponding position of the current frame and the previous frame.

3) Build an image pyramid. Construction method: uniform sampling down.

4) Calculate the optical flow. Calculation method: along the pyramid from top to bottom, the light flow of the upper layer through the interpolation method to the next layer, as the initial value of the next layer, and recursively to finally obtain high precision light flow.

5) Draw the optical flow of the image pixels.

4. Interpretation

4.1. Experimental Installation

The experimental flow channel and the simulation flow channel are consistent. The skin trusteeship speed measurement is set at a hydraulic diameter after the

rectifier plate, and the air volume is adjusted by the frequency conversion fan. Tracer particles were loaded at the inlet of the primary guide blade before the test blade, the measuring blade top gap area was illuminated with a sheet light source laser, and the feasibility and uniformity of tracer particle loading were evaluated. The lighting laser is a dual-pulse Nd: YAG laser from Newwave, model SOLO PIV, as shown in Figure 1. The single pulse was rated at 120 mJ with a pulse width of 5 ns. The laser is able to control the time interval between continuous pulses through the PTU. The laser wavelength of the laser output is 532 nm, and the emitted circular Gaussian laser beam is transmitted to the light test road of the system through the light guide arm. The tracer particle image recording camera is the Lavision PIV system camera of image ProPlus. The experimental device is shown in Figure 1.

4.2. Flow Field Test Results

Since the optical flow method is suitable for calculating the small displacement flow field, the high-resolution CCD camera was selected to shorten the shooting interval of each frame to reduce the inter-frame displacement. The distribution diagram of tracer particles is shown in the following Figure 2.

The flow field obtained by the cross-correlation algorithm is shown in the following Figure 3.

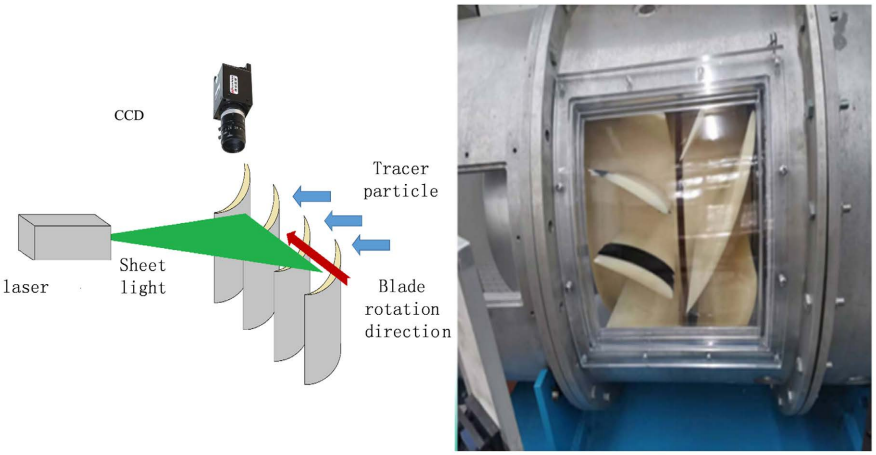

Figure 1. Experimental setup diagram.

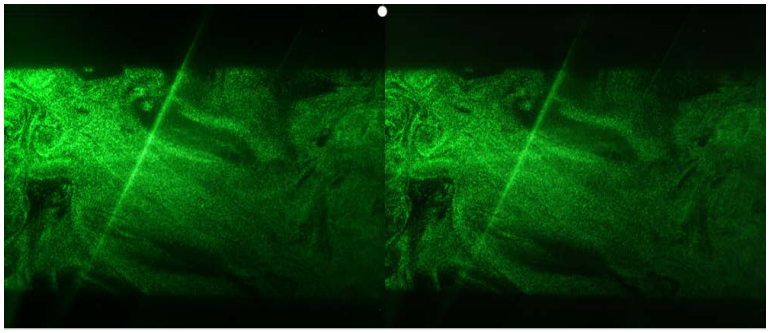

Figure 2. Distribution of the tracer particles.

The resulting velocity field is shown in Figure 4.

The streamline diagram of the movement of the trace particles is shown in Figure 5.

The results obtained by the optical flow algorithm with small displacement are similar to the results obtained by the cross-correlation algorithm, but the optical flow algorithm is much higher than that in terms of accuracy. To verify the accuracy of the optical flow algorithm, the results are also compared with the current world standard particle image velocity measurement software, PIVlab. The results obtained by PIVlab calculation are shown in Figure 6.

It can be seen that the method and the standard test results resolution, but the accuracy of the particle image speed measurement based on optical flow method is significantly less than the traditional particle image speed measurement.

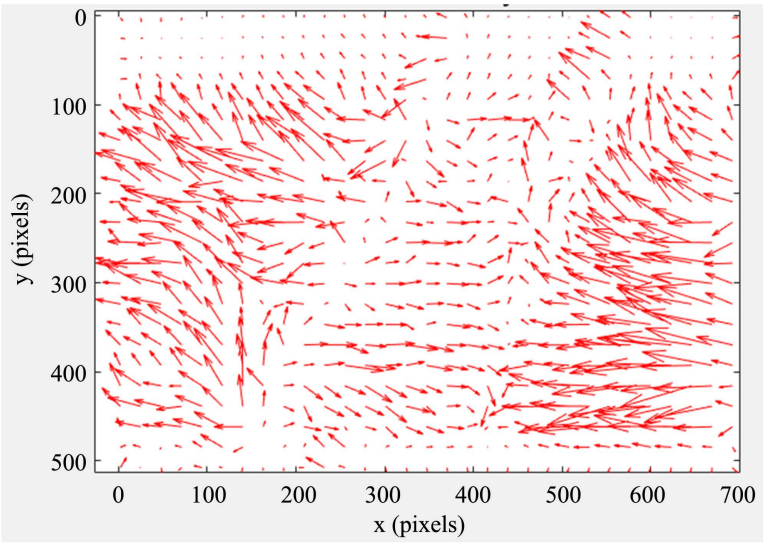

Figure 3. The flow field obtained from the cross-correlation algorithm.

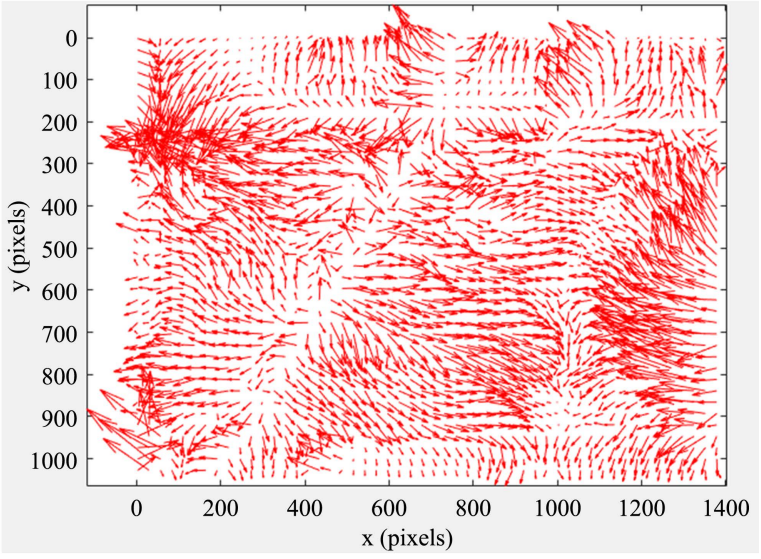

Figure 4. Velocity field.

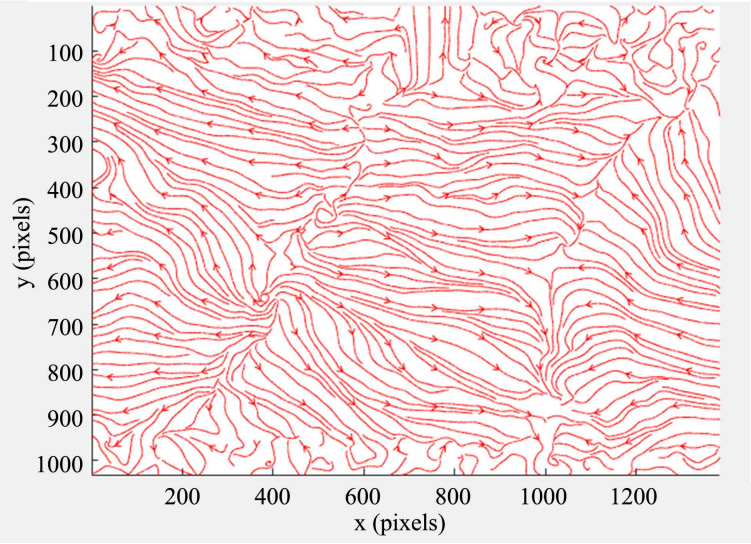

Figure 5. Streamline diagram.

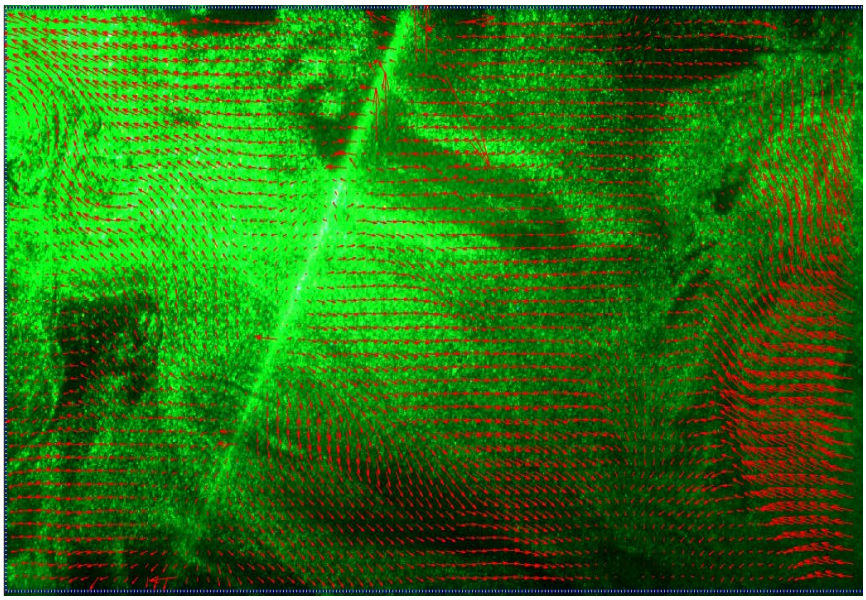

Figure 6. Results obtained by PIVlab.

5. Conclusion

In this paper, the particle image velocimetry based on the optical flow algorithm improves the disadvantages of low resolution and large error based on the cross-correlation algorithm, by constructing a Gaussian pyramid to perform the optical flow calculation, a high resolution optical flow field is obtained. However, the method cannot be measured accurately. The cross-correlation algorithm and optical flow algorithm can be combined. First, the cross-correlation algorithm and the cross-correlation algorithm can calculate the initial flow field through the cross-correlation function and track the displacement field. Then, the optical flow field can be calculated as the double-flow field to supplement the cross-correlation flow field, so as to achieve faster tracking particle tracking detection. However, the

traditional optical flow algorithm is only applicable to calculate the motion with small displacement and requires a high CCD camera. To solve this problem, the advantages of high-resolution and cross-correlation algorithms suitable to calculate large displacements are yet to be explored.

Conflicts of Interest

The author declares no conflicts of interest regarding the publication of this paper.

References

[1] Zhou, S. and Liu, Y. (2003) Numerical Calculation of Three-dimensional Turbulent Flow in MPC Exhaust System of Diesel Engine. *Journal of Harbin Engineering University*, **24**, 5.

[2] Liu, Y., Yang, X.T. and Ma, X.Z. (2012) Flow Field Test Technique Based on Laser Doppler Velocimetry. *Laser and IR*, **42**, 18-21.

[3] McKeown, D.M., McVay, C.A. and Lucas, B.D. (1986) Stereo Verification in Aerial Image Analysis. *Optical Engineering*, **25**, Article ID: 253333. https://doi.org/10.1117/12.7973830

[4] Théo, B., *et al.* (2021) Vision-Based Correspondence Using Relaxation Algorithms for Particle Tracking Velocimetry. *Measurement Science and Technology*, **32**, Article ID: 025303. https://doi.org/10.1088/1361-6501/abb437

[5] Tang, T., Deniz, E., Khokha, M.K. and Tagare, H.D. (2019) Gaussian Process Post-Processing for Particle Tracking Velocimetry. *Biomedical Optics Express*, **10**, 3196-3216. https://doi.org/10.1364/BOE.10.003196

[6] Bao, X.L. and Li, M.G. (2011) A Modified FFT-Based PIV Cross-Correlation Algorithm. *Journal of Dalian University of Technology*, **51**, 417-421.

[7] Nie, M.Y. and Pan, C. (2020) Application of Improved Mixed Ant Colony Algorithm in 3D PTV Matching Algorithm. *Summary Collection of the* 11*th National Academic Conference on Fluid Mechanics*.

[8] James, J.G. (1953) The Perception of the Visual World. *Philosophy of Science*, **20**, 166.

[9] Hartmann, C., Wang, J., Opristescu, D. and Volk, W. (2018) Implementation and Evaluation of Optical Flow Methods for Two-Dimensional Deformation Measurement in Comparison to Digital Image Correlation. *Optics and Lasers in Engineering*, **107**, 127-141. https://doi.org/10.1016/j.optlaseng.2018.03.021

[10] Ruhnau, P., Kohlberger, T., Schnörr, C. and Nobach, H. (2005) Variational Optical Flow Estimation for Particle Image Velocimetry. *Experiments in Fluids*, **38**, 21-32. https://doi.org/10.1007/s00348-004-0880-5

[11] Wu, H., Zhao, R.H., Gan, X.T. and Ma, X.Y. (2019) Measuring Surface Velocity of Water Flow by Dense Optical Flow Method. *Water*, **11**, Article 2320. https://doi.org/10.3390/w11112320

[12] Liu, J., Song, N., Pan, J.X., Abdulr, G. and Yang, M. (2022) A Dense Reconstruction Algorithm for a Sparse Light Field Based on the Optical Flow Method. *CT Theory and Applied Research*, **31**, 173-185.

[13] Zheng, L. and Wang, Z.N. (2022) 3D Tracking Registration Based on Pyramid Optical Flow. *Internet of Things Technology*, **12**, 85-89.